Large magnetoresistance and Fermi surface topology of PrSb

F. Wu,[1] C. Y. Guo,[1] M. Smidman,[1] J. L. Zhang,[2] and H. Q. Yuan[1,3,*]

[1]*Center for Correlated Matter and Department of Physics, Zhejiang University, Hangzhou 310058, China*

[2]*Anhui Province Key Laboratory of Condensed Matter Physics at Extreme Conditions, High Magnetic Field Laboratory of the Chinese Academy of Sciences, Hefei 230031, Anhui, China*

[3]*Collaborative Innovation Center of Advanced Microstructures, Nanjing 210093, China*

(Received 20 June 2017; published 13 September 2017)

We report magnetotransport measurements of PrSb in high magnetic fields. Our results show that PrSb exhibits large magnetoresistance at low temperatures. Meanwhile angle-dependent magnetoresistance measurements were used to probe the Fermi surface via Shubnikov–de Haas oscillations. We found that the angular dependence of the oscillation frequency of the α branch can be explained well by a model for a two-dimensional-like Fermi surface, whereas the effective mass of this branch as a function of angle shows a fourfold signature. The evolution of the Fermi surface with increasing magnetic field also was studied up to 32 T. A continuous increase in the oscillation frequency up to 14 T is observed before it becomes constant at higher fields. Meanwhile our analysis of the residual Landau index from the high-field data reveals a zero Berry phase and therefore trivial topology of the Fermi surface.

DOI: 10.1103/PhysRevB.96.125122

I. INTRODUCTION

Materials with nontrivial electronic band structures have been studied intensively in recent years [1–4]. For instance, topological insulators are bulk insulators, but as a consequence of the topology of the electronic bands, the surface states are gapless [1,5], whereas in Dirac and Weyl semimetals [3,4,6–10], the symmetry protected bands have linear crossings with massless excitations. Topologically nontrivial band structures can lead to distinctive transport behaviors, such as a π Berry phase from the Landau index analysis [11–13], an extremely large magnetoresistance (XMR) [6,7,14,15], and in Weyl semimetals the chiral anomaly can cause a negative longitudinal magnetoresistance (MR) [7,10].

Recently, the observation of XMR in the X(Sb,Bi) series of compounds, where X is a rare-earth element, has attracted much attention [16–29]. In these materials the temperature dependence of the resistivity has a plateau at low temperatures upon applying a magnetic field. In LaSb, it was suggested that this behavior has a similar origin to that of SmB_6 where it is proposed to be related to the appearance of the surface state [16]. However, angle-resolved photoemission spectroscopy (ARPES) measurements provide evidence that the band topology in LaSb is trivial [17]. Meanwhile for LaBi, ARPES measurements show multiple Dirac cones near the Fermi level, and it is proposed to show a nontrivial band topology with a π Berry phase [20,21,26]. In CeSb, a negative longitudinal magnetoresistance was observed, which provides evidence for the presence of the chiral anomaly in the field-induced ferromagnetic state due to time-reversal symmetry breaking [22]. Consequently it is of interest to explore how the topology and Fermi surface evolve upon changing the f-electron configuration in this series of compounds. In addition, since X(Sb,Bi) materials all have moderately high quantum oscillation frequencies, it is important to extend the MR measurements to higher fields in order to reliably determine the Berry phases.

PrSb has a simple cubic rock-salt structure similar to other X(Sb,Bi) materials and has a paramagnetic ground state without any magnetic transitions [30,31]. The trivalent Pr^{3+} ions have a $4f^2$ configuration that results in a large local moment at the Pr site [32], which contributes to the large magnetic-field-induced moments revealed by magnetization measurements [33]. Crystal-field splitting leads to a singlet ground state, and the anisotropic exchange gives rise to singlet-singlet excitations at low temperatures near the X point [31,34]. Previous de Haas–van Alphen effect studies indicate that the extremal cross-sectional areas of the electron orbits become larger with increasing field, resulting in a nonlinear relationship between the number of filled Landau levels and the inverse magnetic field [33,35].

Here we present a detailed magnetotransport study on PrSb. A large magnetoresistance which reaches $\rho(H)/\rho(0) \approx 4300$ at 32 T is observed. To probe the Fermi surface via the Shubnikov–de Haas (SdH) effect, angular-dependent MR measurements are reported. The angular dependence of the quantum oscillation frequency corresponding to the α branch shows a possible two-dimensional- (2D-) like nature of the corresponding Fermi surface. Meanwhile, a fourfold symmetric variation of the effective mass is detected. A detailed analysis of the quantum oscillations indicates an enlargement of the α orbit with increasing field, which becomes nearly constant when the field exceeds 14 T. The analysis of the Landau index of this enlarged orbit shows that at high fields the Fermi surface of PrSb is topologically trivial.

II. EXPERIMENTAL DETAILS

Single crystals of PrSb were synthesized using a flux method described in Ref. [36]. The mixture of Pr, Sb, and Sn elements in a molar ratio of 1:1:10 were cooled slowly from 1100 °C down to 780 °C before centrifuging to remove the Sn flux. The resulting crystals were cubic with a typical length of 3 mm.

Resistivity and angle-dependent magnetoresistance measurements were performed using a Quantum Design Physical

*hqyuan@zju.edu.cn

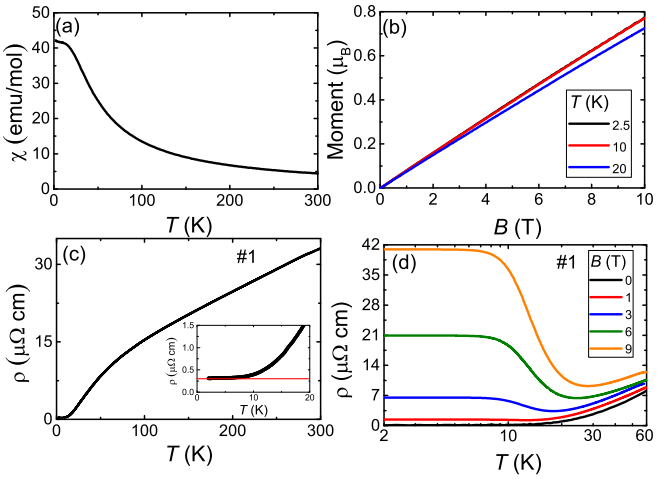

FIG. 1. (a) Temperature dependence of the magnetic susceptibility of PrSb in an applied field of 0.1 T. (b) Magnetization as a function of applied field at three temperatures up to a field of 10 T. (c) Temperature dependence of the resistivity of PrSb sample No. 1 from 300 to 2 K. The inset displays an enlargement of the low-temperature region. (d) Temperature dependence of the resistivity of sample No. 1 in several applied magnetic fields.

Property Measurement System (PPMS) from 300 to 2 K with a maximum applied field of 9 T using a field rotation option. Four Pt wires were attached to the sample by spot welding, and the current was applied parallel to the [100] direction. Magnetic susceptibility measurements were performed using both a Quantum Design superconducting quantum interference device magnetometer and the vibrating sample magnetometer option for the PPMS. The low-temperature magnetoresistance was measured in a ^{3}He system with base temperature of 0.27 K and a maximum applied magnetic field of 15 T. The high-field magnetoresistance measurements were performed at the High Magnetic Field Laboratory of the Chinese Academy of Sciences.

III. RESULTS AND DISCUSSION

Figure 1(a) displays the temperature-dependent magnetic susceptibility of PrSb where there is a broad shoulder at around 10 K, which is consistent with previous reports [37]. The low-temperature behavior can be explained by the crystal-field effect commonly observed in Pr-based Van Vleck paramagnets, such as $PrPt_4Ge_{12}$ [38]. No long-range magnetic ordering is found down to 2 K, and by fitting using the Curie-Weiss law above 50 K, an effective magnetic moment of $\mu_{\rm eff} = 3.3\mu_B$ and a Curie-Weiss temperature of $\Theta_P = -5$ K are obtained. These values are close to the previous study [30] and suggest a trivalent nature of the Pr atoms with two fully localized f electrons. The field-dependent magnetization measurements shown in Fig. 1(b) reveal a nearly linear field dependence of the magnetization at different temperatures below 20 K. At 10 T the magnetization reaches 0.8 μ_B/Pr, consistent with a magnetic moment of $0.9\mu_B$ at 10 T and 15 K [39]. The resistivity of PrSb from 300 to 2 K is presented in Fig. 1(c), which shows typical metallic behavior in zero applied field. The enlarged view of the low-temperature range in the inset shows no anomaly arising from the superconducting transition of Sn, indicating a lack of residual flux in the samples. The residual resistivity is about 0.3 $\mu\Omega$ cm, and the residual resistance ratio is about 110, indicating the high quality of the crystals. Figure 1(d) displays the temperature dependence of the resistivity when different magnetic fields are applied perpendicular to the current. Unlike in zero field where simple metallic behavior is observed, in the presence of a magnetic field there is an increase in the resistivity upon lowering the temperature, which saturates below 10 K. Similar behavior has also been reported in LaSb [16] and YSb [29]. Although in LaSb this behavior was reported to be analogous to the topological Kondo insulator SmB_6, further studies concluded that this plateau is more likely due to electron-hole compensation [17].

We also performed magnetoresistance measurements at various temperatures with fields applied at different angles θ to the current direction (along [100]) as illustrated in Fig. 2(a). Figure 2(a) also displays the MR at $\theta \sim 86^\circ$ at several temperatures, which shows a large MR similar to other XSb compounds where the MR exceeds 300 at 2 K and 9 T. Upon rotating the magnetic field towards the current direction, the MR decreases, but no negative MR is observed, and therefore there is no indication of a chiral anomaly, unlike CeSb where such evidence was found [22]. Upon rotating the sample, we studied the angular dependence of the oscillation frequency and effective mass. As the frequency of the quantum oscillations is proportional to the extremal cross-sectional areas of the Fermi surface, the change in oscillation frequency with angle reflects the Fermi surface structure. The FFT analysis of the SdH quantum oscillations for two values of θ are shown in Fig. 2(c). At $\theta \sim 86^\circ$, the FFT analysis reveals a fundamental frequency of $F_\alpha \sim 220$ T and two harmonic frequencies. At $\theta \sim 42^\circ$, the FFT analysis yields two fundamental α-band frequencies at $F_\alpha \sim 280$ and $F_{\alpha'} \sim 320$ T as well as harmonic frequencies. In addition, there are frequencies associated with the β and γ bands, $F_\beta \sim 463$ and $F_\gamma \sim 934$ T. Note that the β frequency can only be observed clearly at certain angles due to the overlap with $F_{2\alpha}$ and we focus on the anisotropy of the α band. The oscillation frequencies of the α-band as a function of θ obtained from the FFT are shown in Fig. 2(d). The angular dependence of the oscillation frequencies can be fitted by the expression for a 2D Fermi surface $F = F_0/\cos[\theta - (n\pi/2)]$, where $F_0 \sim 219$ T is the first fundamental frequency. This fitting seems to suggest a 2D nature of the α-band Fermi surface. However, three-dimensional (3D) ellipsoidal pockets with large anisotropy also can produce a pseudo-2D-like character of the Fermi surface. For 3D ellipsoidal Fermi surface pockets, the relation between quantum oscillation frequency and angle can be written as $F \sim \pi ab/\sqrt{\sin^2\theta + (a^2/b^2)\cos^2\theta}$, where a/b characterizes the anisotropy [40]. When $a \gg b$, at sufficiently small angles the equation will be very similar to the 2D description of the angular dependence of the quantum oscillation frequency as was reported for LaBi [19]. Meanwhile the temperature dependence of quantum oscillation amplitudes at two angles are shown in Fig. 2(e). The solid line shows the result of fitting with the LK formula [41], yielding effective masses (m^*) of $0.208m_0$ for $\theta \sim 86^\circ$ and $0.245m_0$ for $\theta \sim 42^\circ$.

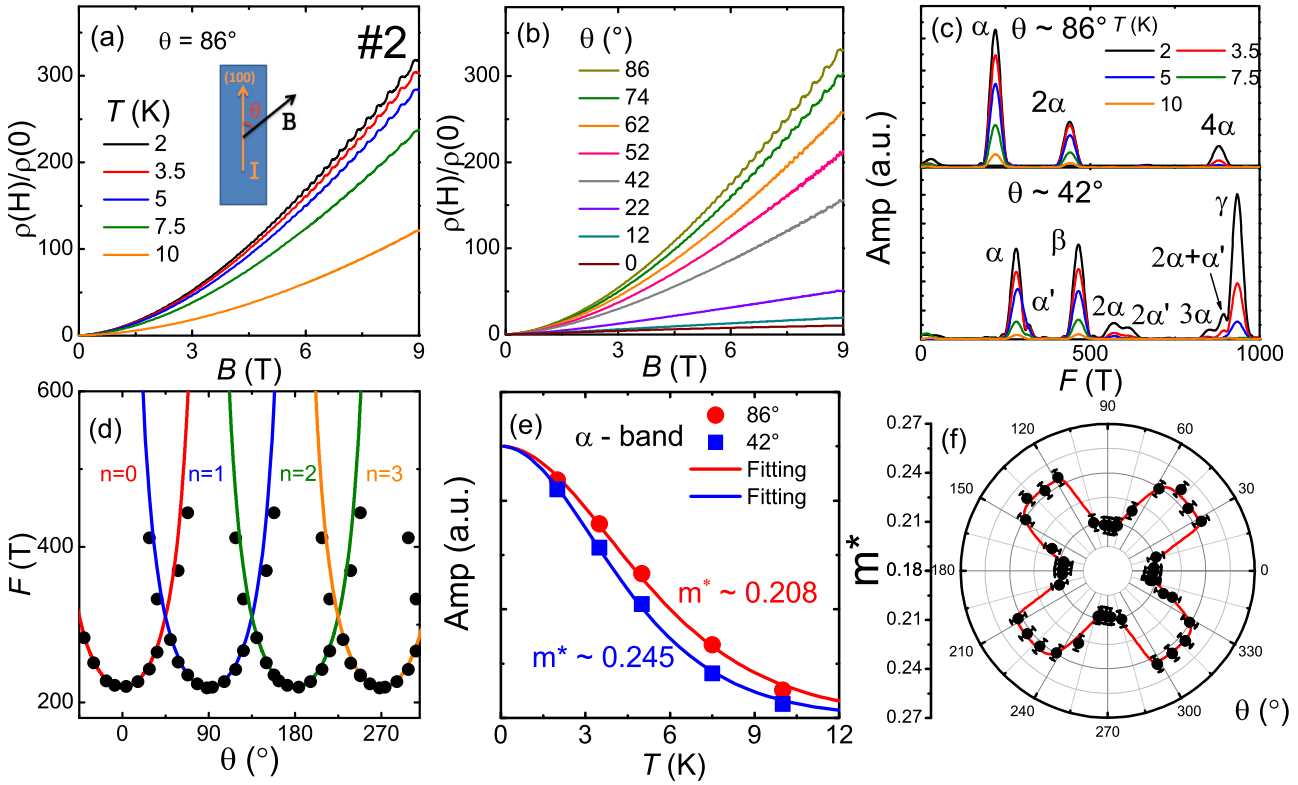

FIG. 2. (a) Field dependence of the resistivity of sample No. 2 at various temperatures with an angle between the magnetic field and the current of $\theta = 86^\circ$. The inset illustrates the experimental configuration. (b) Magnetoresistance at 2 K for different θ's. (c) The fast Fourier-transform (FFT) analysis of the measurements at $\theta \sim 86^\circ$ and 42°. (d) Angular dependence of the SdH oscillation frequencies for the α-band where the field is rotated in the (100) plane. (e) Temperature dependence of the quantum oscillation amplitudes of the α-band for two values of θ, fitted with the Lifshitz-Kosevich (LK) formula. (f) The angular dependence of the effective mass of the α-band obtained from fitting the Lifshitz-Kosevich formula at different θ's.

Moreover, the angular dependence of the effective mass from fitting the LK formula reveals a fourfold signature as shown in Fig. 2(f). Upon rotating the field, there are eight steplike changes in the effective mass, whereas between the steps the value stays at a near constant value. Note that the plateau with a higher effective mass around 45° coincides with where the two bands cross, which leads to an increase in the oscillation frequency. The overall fourfold signature is consistent with the fourfold symmetry of the cubic crystal structure in the (100) plane. The abrupt changes in the effective mass may be related to the structure of the bulletlike Fermi surfaces corresponding to the α-band found in other XSb materials [19,29], which lie perpendicularly in the Brillouin zone, but detailed calculations are required explain this behavior.

To determine whether the large magnetoresistance of PrSb is related to the topological nature of the Fermi surface, we performed high-field magnetoresistance measurements on PrSb. Due to the high frequencies of the quantum oscillations, there can be a reasonably large uncertainty in the extrapolated residual Landau index if the measurements are not performed for sufficiently large fields (small $1/B$). Therefore we measured the SdH oscillations in high magnetic fields to accurately determine the Berry phase. Figure 3(a) displays the transverse magnetoresistance measured at low temperatures down to 0.3 K up to 15 T, whereas Fig. 3(b) shows the transverse magnetoresistance measured up to 32 T. The current is along the [100] direction whereas the magnetic field is perpendicular to the current direction. Large transverse MR

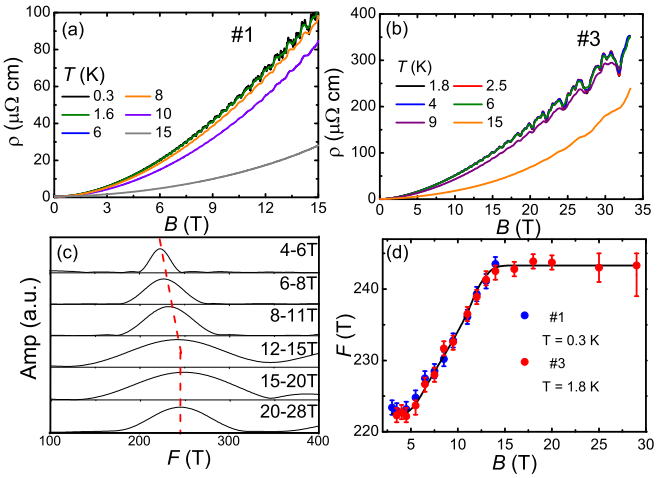

FIG. 3. The magnetoresistance at different temperatures is shown up to a maximum field of (a) 15 and (b) 32 T for samples Nos. 1 and 3, respectively. (c) FFT of quantum oscillations at 1.8 K in different field ranges showing the position of the fundamental frequency of the α-band F_α. (d) F_α as a function of applied field for measurements of two samples.

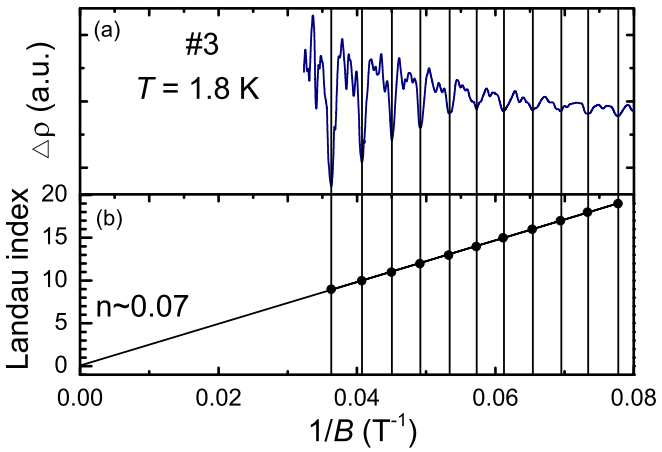

FIG. 4. (a) SdH oscillations of PrSb sample No. 3 at 1.8 K as a function of $1/B$, obtained from subtracting the background contribution. (b) The $1/B$ dependence of the Landau index, obtained from the valley positions of the SdH oscillations. The solid line shows a linear fit, which reveals a residual Landau index of $n = 0.07$.

is observed with clear quantum oscillations, where $\rho(H)/\rho(0)$ is about 4300 at $B = 32$ T. The field-dependent resistivity shows a quadratic dependence, suggesting that electron-hole compensation is the origin of the large MR [42]. Figure 3(c) shows the FFT analysis of the SdH oscillation frequencies of sample No. 3 in different field ranges at 1.8 K. It can be seen that in the lower-field ranges, the oscillation frequency of the α-band increases with increasing magnetic field. The field dependence of these frequencies is displayed in Fig. 3(d) for both samples where the field is taken as the midpoint of the field ranges of the FFT. Whereas an increase in the frequency with a field was reported previously from a comparison between two field ranges [33,35], here we report the detailed evolution. Our results show that there is an increase in the frequency with increasing field up to around 14 T, whereas at larger fields the frequency is nearly unchanged. The origin of this increase in frequency is currently not resolved, but it may correspond to an enlargement of the α orbit. An alternative cause of a change in oscillation frequency is that since quantum oscillations are periodic in $1/B$ rather than $1/H$, the frequencies may be influenced by changes in the magnetization. However, since the magnetization of PrSb is small, the total change in frequency would be less than 1% after making the correction. This small change cannot account for the frequency change observed in PrSb, which is larger than 8% within the field range of 5 to 14 T. Zeeman splitting of the bands by the applied field also can lead to a change in frequency, but in our measurements we do not observe any splitting of the frequencies, and for this scenario it is difficult to account for the constant behavior at higher fields.

Since the oscillation frequency increases with increasing field up to 14 T, the residual value cannot be obtained from a linear fit to the inverse field dependence of the Landau index in this field range. Therefore we analyzed the Landau index at higher fields where the quantum oscillation frequency remains constant. After subtracting the background contribution, the data at 1.8 K above 15 T in Fig. 3(b) were plotted as a function of $1/B$ as displayed in Fig. 4(a). Despite the strong harmonic oscillations, the positions of the valleys can clearly be resolved, and the positions are marked by the vertical lines. Integer Landau levels were assigned to the valley positions, which are shown in Fig. 4(b). From fitting the data with a linear relationship, the residual Landau index was determined to be 0.07, which corresponds to a zero Berry phase [11], and hence the Fermi surface of PrSb in this field range is topologically trivial. Our measurements were measured to sufficiently high fields to measure the ninth Landau index, and therefore the uncertainty associated with the fitted residual value is small, and the results are reliable.

IV. CONCLUSION

To summarize, we report a detailed angle-dependent magnetotransport study of PrSb where we find large MR with $\rho(H)/\rho(0) \approx 4300$ at 32 T. We probed the structure of the Fermi surface via SdH measurements where we observe fourfold symmetry in the angular dependence of the effective mass of the α-band, which shows several abrupt changes. In addition, there is an increase in the quantum oscillation frequencies of the α-band with a magnetic field up to 14 T, indicating an enlargement of the α orbit before reaching a near constant level above 14 T. The analysis of the Landau index at high fields shows that there is a zero Berry phase in this field range, and therefore the Fermi surface topology is trivial. Meanwhile the transverse magnetoresistance shows a near quadratic field dependence, and therefore these results indicate that the large MR in PrSb is more likely due to electron-hole compensation rather than topological protection of the surface state. Whether the band topology remains trivial when no magnetic field is applied remains to be determined, which needs to be checked using ARPES measurements. Furthermore, the origin of the widely observed XMR behavior in this series of compounds is still under debate, and the role of the lanthanide elements in influencing the properties and topology of the band structure needs to be explored further.

ACKNOWLEDGMENTS

We thank Y. Liu, C. Cao, and X. Lu for valuable discussions and helpful suggestions. This work was supported by the National Key R&D Program of China (Grants No. 2017YFA0303100 and No. 2016YFA0300202), the National Natural Science Foundation of China (Grants No. U1632275 and No. 11474251), and the Science Challenge Project of China (Project No. TZ2016004).

[1] M. Z. Hasan and C. L. Kane, *Colloquium*: Topological insulators, Rev. Mod. Phys. **82**, 3045 (2010).

[2] X.-L. Qi and S.-C. Zhang, Topological insulators and superconductors, Rev. Mod. Phys. **83**, 1057 (2011).

[3] Z. K. Liu, B. Zhou, Y. Zhang, Z. J. Wang, H. M. Weng, D. Prabhakaran, S.-K. Mo, Z. X. Shen, Z. Fang, X. Dai, Z. Hussain, and Y. L. Chen, Discovery of a three-dimensional topological Dirac semimetal, Na_3Bi, Science **343**, 864 (2014).

[4] H. Weng, C. Fang, Z. Fang, B. A. Bernevig, and X. Dai, Weyl Semimetal Phase in Noncentrosymmetric Transition-Metal Monophosphides, Phys. Rev. X **5**, 011029 (2015).

[5] Y. L. Chen, J. G. Analytis, J.-H. Chu, Z. K. Liu, S.-K. Mo, X. L. Qi, H. J. Zhang, D. H. Lu, X. Dai, Z. Fang *et al.*, Experimental realization of a three-dimensional topological insulator, Bi_2Te_3, Science **325**, 178 (2009).

[6] T. Liang, Q. Gibson, M. N. Ali, M. Liu, R. J. Cava, and N. P. Ong, Ultrahigh mobility and giant magnetoresistance in the Dirac semimetal Cd_3As_2, Nat. Mater. **14**, 280 (2015).

[7] X. Huang, L. Zhao, Y. Long, P. Wang, D. Chen, Z. Yang, H. Liang, M. Xue, H. Weng, Z. Fang *et al.*, Observation of the Chiral-Anomaly-Induced Negative Magnetoresistance in 3D Weyl Semimetal TaAs, Phys. Rev. X **5**, 031023 (2015).

[8] Y. Luo, N. J. Ghimire, M. Wartenbe, H. Choi, M. Neupane, R. D. McDonald, E. D. Bauer, J. Zhu, J. D. Thompson, and F. Ronning, Electron-hole compensation effect between topologically trivial electrons and nontrivial holes in NbAs, Phys. Rev. B **92**, 205134 (2015).

[9] X. Wan, A. M. Turner, A. Vishwanath, and S. Y. Savrasov, Topological semimetal and Fermi-arc surface states in the electronic structure of pyrochlore iridates, Phys. Rev. B **83**, 205101 (2011).

[10] M. Hirschberger, S. Kushwaha, Z. Wang, Q. Gibson, S. Liang, C. A. Belvin, B. A. Bernevig, R. J. Cava, and N. P. Ong, The chiral anomaly and thermopower of Weyl Fermions in the half-Heusler GdPtBi, Nat. Mater. **15**, 1161 (2016).

[11] G. P. Mikitik and Y. V Sharlai, Manifestation of Berry's Phase in Metal Physics, Phys. Rev. Lett. **82**, 2147 (1999).

[12] Y. Zhang, Y.-W. Tan, H. L. Stormer, and P. Kim, Experimental observation of the quantum Hall effect and Berry's phase in graphene, Nature (London) **438**, 201 (2005).

[13] H. Murakawa, M. S. Bahramy, M. Tokunaga, Y. Kohama, C. Bell, Y. Kaneko, N Nagaosa, H. Y. Hwang, and Y. Tokura, Detection of Berry phase in a bulk Rashba semiconductor, Science **342**, 1490 (2013).

[14] C. Shekhar, A. K Nayak, Y. Sun, M. Schmidt, M. Nicklas, I. Leermakers, U. Zeitler, Y. Skourski, J. Wosnitza, Z. Liu *et al.*, Extremely large magnetoresistance and ultrahigh mobility in the topological Weyl semimetal candidate NbP, Nat. Phys. **11**, 645 (2015).

[15] M. N. Ali, J. Xiong, S. Flynn, J. Tao, Q. D. Gibson, L. M. Schoop, T. Liang, N. Haldolaarachchige, M. Hirschberger, N. P. Ong *et al.*, Large, non-saturating magnetoresistance in WTe_2, Nature (London) **514**, 205 (2014).

[16] F. F. Tafti, Q. D. Gibson, S. K. Kushwaha, N. Haldolaarachchige, and R. J. Cava, Resistivity plateau and extreme magnetoresistance in LaSb, Nat. Phys. **12**, 272 (2015).

[17] L.-K. Zeng, R. Lou, D.-S. Wu, Q. N. Xu, P.-J. Guo, L.-Y. Kong, Y.-G. Zhong, J.-Z. Ma, B.-B. Fu, P. Richard, P. Wang, G. T. Liu, L. Lu, Y.-B. Huang, C. Fang, S.-S. Sun, Q. Wang, L. Wang, Y.-G. Shi, H. M. Weng, H.-C. Lei, K. Liu, S.-C. Wang, T. Qian, J.-L. Luo, and H. Ding, Compensated Semimetal LaSb With Unsaturated Magnetoresistance, Phys. Rev. Lett. **117**, 127204 (2016).

[18] M. Zeng, C. Fang, G. Chang, Y.-A. Chen, T. Hsieh, A. Bansil, H. Lin, and L. Fu, Topological semimetals and topological insulators in rare earth monopnictides, arXiv:1504.03492.

[19] N. Kumar, C. Shekhar, S.-C. Wu, I. Leermakers, O. Young, U. Zeitler, B. Yan, and C. Felser, Observation of pseudo-two-dimensional electron transport in the rock salt-type topological semimetal LaBi, Phys. Rev. B **93**, 241106 (2016).

[20] X. H. Niu, D. F. Xu, Y. H. Bai, Q. Song, X. P. Shen, B. P. Xie, Z. Sun, Y. B. Huang, D. C. Peets, and D. L. Feng, Presence of exotic electronic surface states in LaBi and LaSb, Phys. Rev. B **94**, 165163 (2016).

[21] S. Sun, Q. Wang, P.-J. Guo, K. Liu, and H. Lei, Large magnetoresistance in LaBi: Origin of field-induced resistivity upturn and plateau in compensated semimetals, New J. Phys. **18**, 082002 (2016).

[22] C. Y. Guo, C. Cao, M. Smidman, F. Wu, Y. J. Zhang, F. Steglich, F.-C. Zhang, and H. Q. Yuan, Possible Weyl fermions in the magnetic Kondo system CeSb, npj Quantum Mater. **2**, 39 (2017).

[23] N. Wakeham, E. D. Bauer, M. Neupane, and F. Ronning, Large magnetoresistance in the antiferromagnetic semimetal NdSb, Phys. Rev. B **93**, 205152 (2016).

[24] M. Neupane, M. M. Hosen, I. Belopolski, N. Wakeham, K. Dimitri, N. Dhakal, J.-X. Zhu, M. Z. Hasan, E. D. Bauer, and F. Ronning, Observation of Dirac-like semi-metallic phase in NdSb, J. Phys.: Condens. Matter **28**, 23LT02 (2016).

[25] Y. Wang, Y. Wang, C. Y. Xi, L. S. Ling, S. L. Zhang, L. He, T. Han, H. Han, J. Yang, D. Liang, J. Gong, L. Luo, W. Tong, L. Zhang, Z. Qu, Y. Y. Han, W. K. Zhu, L. Pi, C. Zhang, and Y. Zhang, Observations of topological semimetal state and field-induced Fermi surface change in the antiferromagnetic monopnictide NdSb, arXiv:1702.08121.

[26] J. Nayak, S.-C. Wu, N. Kumar, C. Shekhar, S. Singh, J. Fink, E. E. D. Rienks, G. H. Fecher, S. S. P. Parkin, B. Yan *et al.*, Multiple Dirac cones at the surface of the topological metal LaBi, Nat. Commun. **8**, 13942 (2017).

[27] F. F. Tafti, Q. Gibson, S. Kushwaha, J. W. Krizan, N. Haldolaarachchige, and R. J. Cava, Temperature-field phase diagram of extreme magnetoresistance, Proc. Natl. Acad. Sci. USA **113**, E3475 (2016).

[28] P.-J. Guo, H.-C. Yang, B.-J. Zhang, K. Liu, and Z.-Y. Lu, Charge compensation in extremely large magnetoresistance materials LaSb and LaBi revealed by first-principles calculations, Phys. Rev. B **93**, 235142 (2016).

[29] O. Pavlosiuk, P. Swatek, and P. Wiśniewski, Giant magnetoresistance, three-dimensional Fermi surface and origin of resistivity plateau in YSb semimetal, Sci. Rep. **6**, 38691 (2016).

[30] T. Tsuchida and W. E. Wallace, Magnetic characteristics of compounds of Cerium and Praseodymium with Va elements, J. Chem. Phys. **43**, 2885 (1965).

[31] B. Lüthi, M. E. Mullen, and E. Bucher, Elastic Constants in Singlet Ground-State Systems: PrSb and Pr, Phys. Rev. Lett. **31**, 95 (1973).

[32] C. Vettier, D. B. McWhan, E. I. Blount, and G. Shirane, Pressure Dependence of Magnetic Excitations in PrSb, Phys. Rev. Lett. **39**, 1028 (1977).

[33] G. Kido, K. Komorita, Y. Nakagawa, and T. Suzuki, De Haas-van Alphen effect and high-field magnetization in PrSb singlet-ground-state systems, J. Magn. Magn. Mater. **104**, 1239 (1992).

[34] D. B. McWhan, C. Vettier, R. Youngblood, and G. Shirane, Neutron scattering study of pressure-induced antiferromagnetism in PrSb, Phys. Rev. B **20**, 4612 (1979).

[35] A. Kido, S. Nimori, G. Kido, Y. Nakagawa, Y. Haga, and T. Suzuki, De Haas-van Alphen effect and anisotropic

magnetization of singlet ground state PrSb in high magnetic field, Physica B: Condens. Matter **186**, 185 (1993).

[36] P. C. Canfield and Z. Fisk, Growth of single crystals from metallic fluxes, Philos. Mag. B **65**, 1117 (1992).

[37] P. Monachesi, Z. Domański, and M. S. S. Brooks, Optical and magneto-optical properties of PrSb, Phys. Rev. B **50**, 1013 (1994).

[38] M. Toda, H. Sugawara, K. Magishi, T. Saito, K. Koyama, Y. Aoki, and H. Sato, Electrical, magnetic and NMR studies of Ge-based filled skutterudites $R\mathrm{Pt_4Ge_{12}}(R = \mathrm{La,Ce,Pr,Nd})$, J. Phys. Soc. Jpn. **77**, 124702 (2008).

[39] J. Schoenes, H. Brändle, A. Weber, and F. Hulliger, Magneto-optical properties of PrSb, Physica B: Condens. Matter **163**, 496 (1990).

[40] J. M. Schneider, B. A. Piot, I. Sheikin, and D. K. Maude, Using the De Haas-Van Alphen Effect to Map Out the Closed Three-Dimensional Fermi Surface of Natural Graphite, Phys. Rev. Lett. **108**, 117401 (2012).

[41] D. Shoenberg, *Magnetic Oscillations in Metals* (Cambridge University Press, Cambridge, UK, 2009).

[42] A. B. Pippard, *Magnetoresistance in Metals* (Cambridge University Press, Cambridge, UK, 1989), Vol. 2.